LA-10700-MS

UC-10
Issued: January 1987

Materials Compatibility During the Chlorination of Molten $CaCl_2 \cdot CaO$ Salts

LA--10700-MS

DE87 004770

Charles E. C. Rense
Keith W. Fife
David F. Bowersox
Michelle D. Ferran

Los Alamos National Laboratory
Los Alamos, New Mexico 87545

MATERIALS COMPATIBILITY DURING THE CHLORINATION OF MOLTEN $CaCl_2 \cdot CaO$ SALTS

by

Charles E. C. Rense, Keith W. Fife, David F. Bowersox, and Michelle D. Ferran

ABSTRACT

As part of our effort to develop a semicontinuous PuO_2 reduction process, we are investigating promising materials for containing a 900°C molten $CaCl_2 \cdot CaO$ chlorination reaction. We want the material to contain this reaction and to be reusable. We tested candidate materials in a simulated salt (no plutonium) using anhydrous HCl as the chlorinating agent. Data are presented on the performance of 36 metals and alloys, 9 ceramics, and 3 coatings.

INTRODUCTION

The Plutonium Metal Technology Group (MST-13) at Los Alamos National Laboratory routinely performs plutonium metal purification in molten salt systems. One step of this operation involves the pyrochemical reduction of impure plutonium dioxide to plutonium metal.[1-3] The group uses calcium metal in a solvent bath of molten calcium chloride to reduce plutonium dioxide according to the reaction:

$$PuO_2 + 2Ca^{\circ} \xrightarrow[850°C]{CaCl_2} Pu + 2CaO \cdot 11CaCl_2 \quad .$$

Because of the limited solubility of CaO in $CaCl_2$ (18 mol%), our facility cannot reuse these solvent salts and currently discards them after each reduction. Because these spent salts contain low levels of plutonium, we discard them as a low-level waste. Not only is the cost of such disposal high, but the plutonium they contain is lost.

Research into converting this spent solvent salt back to $CaCl_2$ for recycle is well under way. Currently, our staff converts molten $CaCl_2 \cdot CaO$ to $CaCl_2$ by chlorinating the salt mixture. After evaluating potential chlorinating agents, including phosgene, hydrogen chloride, chlorine, ammonium chloride, carbon tetrachloride, magnesium chloride, and zinc chloride, we determined that both hydrogen chloride and chlorine are the most effective in regenerating a synthetic spent salt.[4]

Presently, the direct oxide reduction (DOR) process is a batch operation (Fig. 1). Our technicians load PuO_2,

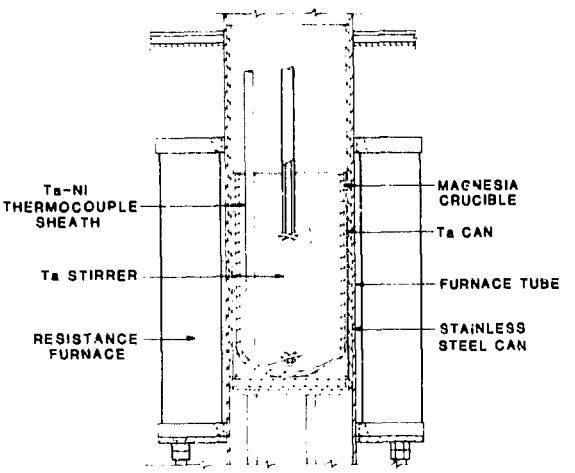

Fig. 1. Equipment for the pyrochemistry recovery of plutonium by direct oxide reduction of plutonium dioxide to plutonium metal.

$CaCl_2$, and calcium metal into a 38-cm-tall, 15-cm-diameter vitrified MgO crucible and heat it to 850°C. After stirring and cooling the reagents, they break away the MgO crucible and recover the metal button.

Waste from the process consists of spent salt and the broken crucible. We hope to obtain up to an 80% reduction in waste volume if regeneration and recycle can be incorporated into the DOR process.

Regeneration and recycle of molten salts have been demonstrated in research settings. Transfer of molten salts from one reaction vessel to another is a necessary aspect of recycle and has been demonstrated. With successful development of these areas, our group could conceivably convert DOR from a batch operation to a semicontinuous process.

To successfully convert DOR from a batch to a semicontinuous process, our group must address the compatibility of construction materials with both DOR and regeneration environments. Below is a list of equipment and the environments it must withstand.

Reduction vessel:	At 900°C, a mixture of $CaCl_2$, CaO, calcium metal, plutonium metal, and PuO_2.
Regeneration vessel:	At 900°C, a mixture of $CaCl_2$-CaO salt, a sparge of either HCl or Cl_2 gas, and some residual plutonium and calcium metal.
Sparge tube:	Same as regeneration vessel.
Transfer tube:	At 900°C, a mixture of $CaCl_2$-CaO salt and some residual plutonium and calcium metal.

Reduction vessels and sparge tubes are presently made of vitrified MgO. Although MgO adequately resists the environment, it is brittle and has only fair thermal shock resistance. If the multiple-run semicontinuous oxide reduction process experienced a broken DOR vessel, then the system would be disrupted and plutonium metal previously produced in the vessels would be lost. A high breakage rate of these vessels in the proposed semicontinuous oxide reduction process would be unacceptable.

Our group identified the issue of materials compatibility early in the concept stage of this semicontinuous DOR process, resulting in the initiation of a materials compatibility test program. The program began in a radioactively cold facility using a synthetic spent salt, which differs from a true salt in its lack of both trace plutonium and calcium metal. Initially, our personnel evaluated candidate materials by visual inspection, weight loss analysis, and chemical analysis of the test batch salt. We eliminated many materials from consideration based upon these criteria. For the metals that appeared to hold up well, we expanded testing and evaluation to include metallographic observation and hardware fabrication and testing. Table I lists the 36 metals and alloys evaluated, and Table II and Table III list the 9 ceramics and the 3 coatings, respectively, which were tested. Each of these three groups is discussed separately under Results and Discussion, with emphasis given to the metals evaluated.

EXPERIMENTAL PROCEDURE

Our procedure was to contact candidate samples with HCl gas in $CaCl_2$ + 10 wt% CaO salt at 900°C. Figure 2 shows the basic apparatus. We nested a platinum crucible in a quartz tube, which was placed in a resistance furnace. A technician then loaded into the platinum crucible 72.0 g of $CaCl_2$ and 8.0 g of CaO. Once the salt was melted and the furnace achieved stable operating temperature, the technician lowered the coupon into the salt and, after injecting argon for 15 min, started an HCl sparge at 0.7 ℓ/min. A run consisted of 1 h of HCl exposure followed by 15 min of argon to purge the system of HCl. After its exposure, the technician pulled the sample coupon out of the salt and took a sample of the salt. A more detailed procedure is listed below.

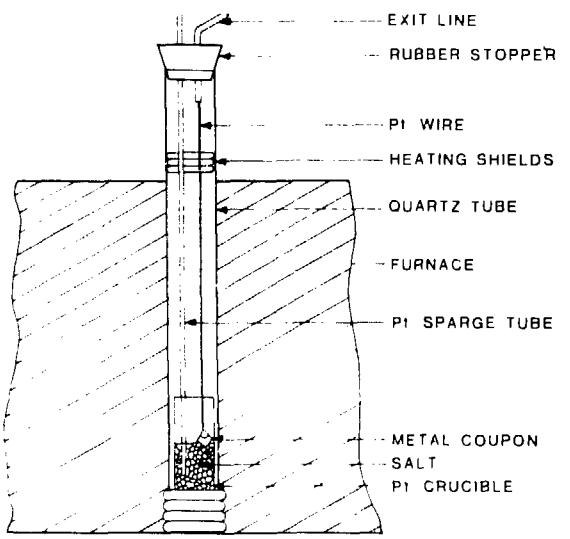

Fig. 2. Test setup used to evaluate candidate materials. Once the salt is melted, the test coupon is submerged in the salt and an HCl sparge is begun.

TABLE I

METALS AND ALLOYS TESTED IN THE $CaCl_2 \cdot CaO$ REGENERATION ENVIRONMENT USING HCl AS THE CHLORINATING AGENT

Nickel Base	"Pure" Metals	Iron Base	Cobalt Base	Refractory Base	Zirconium Base
Allcorr[a]	Cobalt	ASTM 317L	Carpenter L605[b]	ASTM B708	Zirconium 705
Cabot 214[c]	Hafnium (4% Zr)	ASTM A446	MP35N[d]	KBI 40[e]	Zircaloy 4
Hastelloy B2[c]	Molybdenum			Ta-10W	
Hastelloy C276[c]	Nickel			TZM, Arc Cast[e]	
Hastelloy G3[c]	Rhenium			Moly-10Re	
Hastelloy S[c]	Tantalum			Moly-50Re	
Hastelloy X[c]	Titanium				
Inconel 600[f]	Tungsten				
Inconel 601[f]	Zirconium				
Inconel 617[f]					
Inconel 625[f]					
Inconel 690[f]					
Inconel 750[f]					
Inconel 751[f]					
Monel K500[f]					

[a]Teledyne Allvac: Box 759, Monroe, NC 28110
[b]Carpenter Technology Corporation: Reading, PA 19603
[c]Cabot Corporation: 1020 West Park Ave, Kokomo, IN 46901
[d]SPS: P. O. Box 1000, New Town, PA 18940
[e]AMAX: 21801 Tungsten Rd, Cleveland, OH 44117
[f]Inco Alloys International: Huntington, WV 25720

TABLE II

CERAMICS TESTED IN THE $CaCl_2 \cdot CaO$ REGENERATION ENVIRONMENT USING HCl AS THE CHLORINATING AGENT

Thoria
Cesium sulfide
Magnesia + 1 wt% yttria
Magnesia + 3 wt% yttria
Alumina + 2 wt% yttria
Equimoiar magnesia + alumina
Silicon carbide
Zirconia + 15 wt% yttria
Beryllia

TABLE III

COATINGS AND THEIR SUBSTRATES EVALUATED IN $CaCl_2 \cdot CaO$ REGENERATION ENVIRONMENT USING HCl AS THE CHLORINATING AGENT[a]

Coating	Substrate
Erbia (1 mil)	Allcorr
Gold (1-3 mil)	ASTM 317L
Yttria (1 mil)	Hastelloy C276
	Inconel 600
	Inconel 601
	Molybdenum
	Ta-10W
	TZM

[a]All three coatings were tested on all substrates except Ta-10W and TZM, which were tested only with yttria.

1. The test coupon is identified and marked; its dimensions and initial weight are recorded. (Most coupons were appoximately 2 to 3 cm square and from 1 to 5 mm thick.)
2. Weighed and loaded into the platinum crucible is 72 g of $CaCl_2$ and 8 g of CaO.
3. Platinum wire, usually through a hole in a corner of the test coupon, is used to hold and immerse the sample and to remove it from the molten salt.
4. Once the unmelted salt and test coupon are in the furnace (see Fig. 2), the furnace is heated to 900°C with an argon flush applied while the salt is melting. The test coupon is held above the salt.
5. Once temperature is reached and the salt is melted, the test coupon is completely submerged in the salt.
6. The test coupon is subjected to a 15-min argon sparge, followed by an HCl sparge for 1 h, and a final 15-min argon sparge. After this, the test coupon is pulled out of the furnace.
7. After removal of the test coupon, a sample of the salt is obtained by using a quartz tube and pipet bulb.
8. The test coupon is washed and gently cleaned in water and then reweighed and measured.

RESULTS AND DISCUSSION

Metals

Our group evaluated both traditional and exotic metals and their alloys. Compiled in Table IV are the nominal compositions of these alloys. As mentioned previously, our initial criteria for evaluating the performance of these alloys were visual inspection, chemial analysis of the salt bath, and weight loss. Although there are many problems inherent in evaluating corrosion resistance using these criteria, we deemed the volume of samples and the cost in both time and money of more detailed analysis unnecessary for our program. If the test sample showed obvious signs of severe corrosion, the staff eliminated the metal from further consideration. We report weight loss data in grams per square centimeter for each run and as an accumulation over the span of the test. Our analytical group performed chemical analysis of test bath salts after each run and we present these data, along with weight loss data, in Appendix A. Results from the chemical analysis of the salts are helpful in confirming the corrosion behavior of our samples. For example, we see relatively little molybdenum in its salt bath (average of 308 ppm per 1-h

TABLE IV

COMPOSITION OF ALLOYS TESTED IN THE HCl CHLORINATION OF MOLTEN $CaCl_2 \cdot CaO$[a]

Alloy	Composition
Nickel Base	
Allcorr	Ni + 31 Cr, 10 Mo, 2 W
Cabot 214	Ni + 16 Cr, 4.5 Al, 2.5 Fe, Y
Hastelloy B2	Ni + 16 Cr, 15 Mo, 3 Fe, 2 Co, 1 W
Hastelloy C276	Ni + 16 Cr, 15 Mo, 5 Fe, 3.7 W, 1.4 Co, 1 Mn
Hastelloy G3	Ni + 28 Mo, 1.6 Fe, 1 Cr, 1 Co, 1 Mn
Hastelloy S	Ni + 22 Cr, 19.5 Fe, 7 Mo, 5 Co, 1.5 W, Nb
Hastelloy X	Ni + 22 Cr 18.5 Fe, 9 Mo, 1.5 Co
Inconel 600	Ni + 15 Cr, 6 Fe, 1 Mn
Inconel 601	Ni + 23 Cr,14 Fe, 1.5 Al, Mn
Inconel 617	Ni + 22 Cr, 12.5 Co, 9 Mo, 1.5 Fe, 1 Al
Inconel 625	Ni + 20 Cr, 9 Mo, 5 Fe, 4 (Nb + Ta)
Inconel 690	Ni + 30 Cr, 9 Fe
Inconel 750	Ni + 14 Cr, 5 Fe, 2.5 Ti, Nb
Inconel 751	Ni + 14 Cr, 5 Fe, 2 Ti, 1 Al, Nb
Monel K500	Ni + 30 Cu, 3 Al, 1 Fe
Iron Base	
ASTM 317L	Fe + 18.4 Cr, 15.8 Ni, 4.2 Mo, 1.6 Mn, 0.4 Cu
ASTM A446	Fe + 25 Cr, 0.6 Mn, 0.4 Ni
Cobalt Base	
Carpenter L605	Co + 20 Cr, 15 W, 10 Ni
MP35N	Co + 35 Ni, 20 Cr, 10 Mo
Refractory Base	
ASTM B708	Ta + 2.5 W, 0.15 Nb
KBI 40	Ta + 40 Nb
Moly-10Re	Mo + 10 Re
Moly-50Re	Mo + 50 Re
Ta-10W	Ta + 10 W
TZM	Mo + 0.5 Ti, 0.1 Zr
Zirconium Base	
Zircaloy 4	Zr + 4.0 Hf, 1.5 Sb, 0.2 Fe, 0.1 Cr, Oxygen
Zirconium 705	Zr + 2.5 Nb, 4.0 Hf, Oxygen

[a]Actual chemistries are given when known; otherwise, nominal chemistries are listed.

run) compared with the iron pickup seen in the bath testing ASTM 317L (average of 2800 ppm per 4-h run). Chromium appears to be selectively leached from nickel-based alloys.

As the data base was generated, our section fabricated trial regeneration vessels from some of the more promising metals. Vessels made from Inconel 600, Inconel 601, and Cabot 214 were tested. We made and tested regeneration vessels of these three alloys because 1) their corrosion resistance, from initial testing, appeared good, and 2) these are relatively inexpensive and available alloys. Although the vessels held up for several hours of testing, none were sufficiently resistant to the regeneration environment. Concurrent with this testing, our staff initiated metallographic examination of some test coupons.

Metallographic examination included macro views of the test coupons, scanning electron microscope (SEM) views of the cleaned surface (at 100X and 1000X magnification), and an as-polished cross-sectional view to evaluate depth of corrosion. As a comparison of some of the metals evaluated, Fig. 3 shows macro views of molybdenum, MP35N, Inconel 600, and Monel K500. Figure 4 shows SEM views of these alloys, and Fig. 5 shows cross-sectional views.

A comparison of resistance to attack, or stability, can be performed with these photographs. For the four samples seen in Figs. 3 through 5, the order of stability is molybdenum, MP35N, Inconel 600, and Monel K500. Molybdenum's cross section shows very little sign of attack. (The white band along the edge is due to light refraction and is not a feature of the sample itself.) MP35N shows some attack, but not a great amount. Inconel 600's cross section, however, shows fairly deep penetration. Although this cross section shows poor resistance to attack, recall that its outer appearance (Fig. 3) and its weight loss data (Appendix A) indicated fairly good resistance to attack. Monel K500, whose weight loss and appearance indicated poor resistance, indeed shows complete penetration of attack (Fig. 5).

We measured the depth of penetration for these alloys and converted the measurements to depth per year values (millimeters per year). Figure 6 summarizes the penetration data for several alloys.

Ceramics

As with the metal testing, our analytical staff performed chemical analyses on the salt baths used in each ceramic coupon test. Appendix B presents pertinent chemical data, along with weight loss data. Of the ceramics tested to date, none, with the exception of beryllium oxide, showed outstanding resistance to attack. Furthermore, most of the samples had fair to poor thermal shock resistance and cracked after several runs. Beryllium oxide, however, is relatively resistant to thermal shock and, based upon limited weight loss data, showed reasonable resistance to the test environment. Because magnesium oxide is currently being used for the reaction vessels, however, switching to another ceramic may not greatly improve our present system. All of the tested ceramics indicate that breakage rates due to both thermal shock and inherent brittleness will be high.

Coatings

Early in the program, our group applied several coatings to a variety of substrates and tested them in the regeneration environment. These coatings included gold, yttria, and erbia. We did not test platinum because it is incompatible with both plutonium and calcium metal. None of the coatings held up well (Table V). Our staff is presently investigating other coating materials such as MgO and substrates with compatible coefficients of thermal expansion.

CONCLUSIONS AND FUTURE PLANS

A regeneration environment at 900°C of calcium chloride, calcium oxide, and anhydrous HCl is extremely corrosive to the standard engineering materials we have tested.

Of the nickel-based alloys tested (15 total), none were able to satisfactorily withstand this environment. Some evidence exists that chromium is often selectively leached from nickel-based alloys.

Molybdenum, rhenium, and molybdenum/rhenium alloys satisfactorily withstood the tests. However, initial evaluation of these metals with calcium metal present in the salt indicates that calcium may aggressively attack molybdenum.

Ceramics were also unable to resist attack from this environment. Furthermore, their resistance to thermal shock is poor.

Coatings of gold, erbia, and yttria were unable to resist attack. Other coating systems, such as MgO, are still under consideration.

We are altering testing procedures to better reflect actual regeneration environments (adding calcium metal and switching from HCl to Cl_2 as the regenerating gas). We are also devoting more effort to coating systems. A coating of MgO on an acceptable substrate is an attractive system. Because of thermal expansion mismatches, however, our group has not yet found an acceptable substrate. Other corrosion prevention methods, such as cathodic or anodic protection, are being considered.

For semicontinuous DOR to become a reality, our industry must solve these material compatibility problems. If an alternative material cannot be found, we will continue to use MgO for the reaction vessels. Possibly

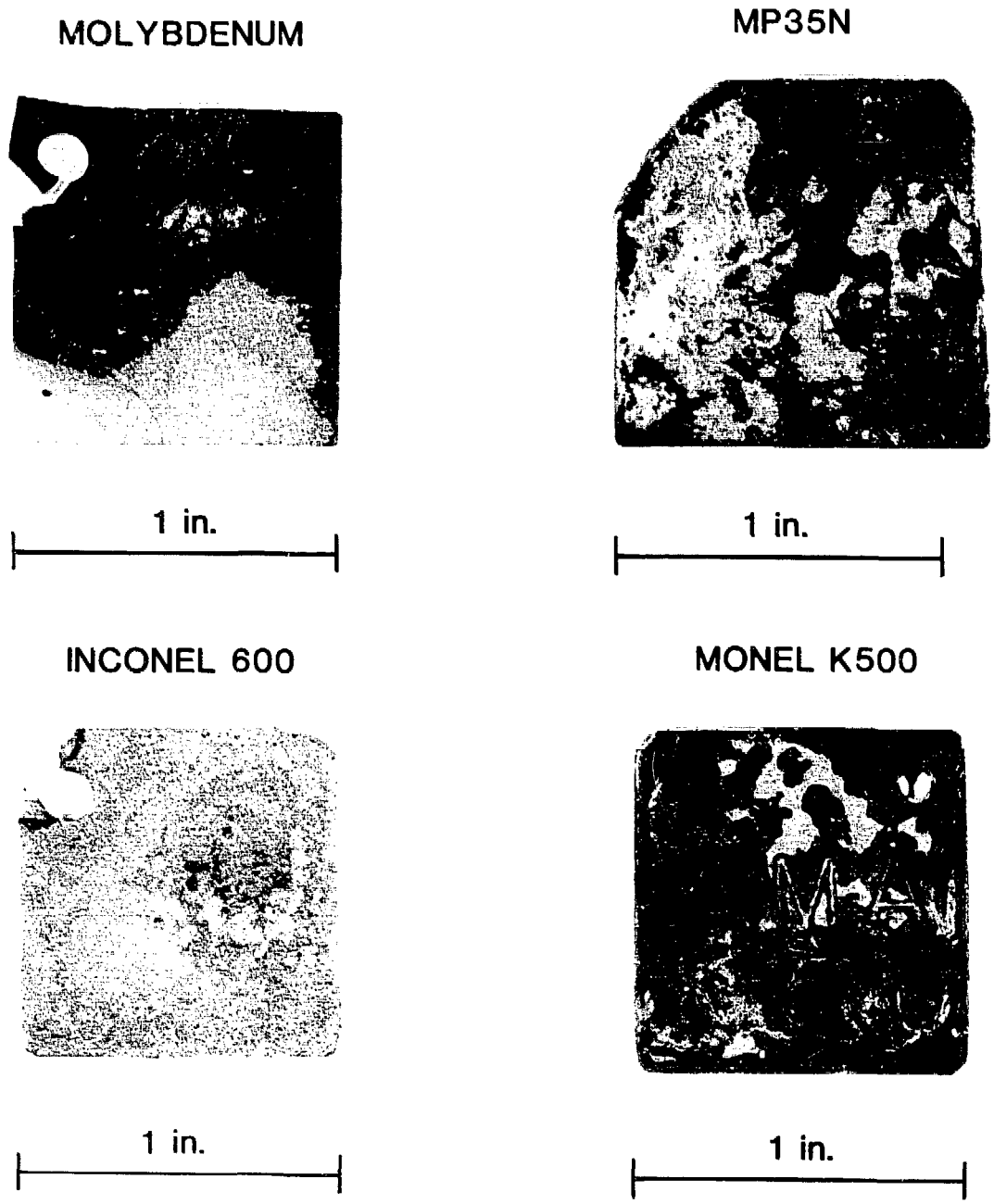

Fig. 3. Macro view of four representative test coupons. Order of decreasing resistance to attack is: Molybdenum, MP35N, (cobalt/nickel base), Inconel 600 (nickel base + chromium), and Monel K500 (nickel base).

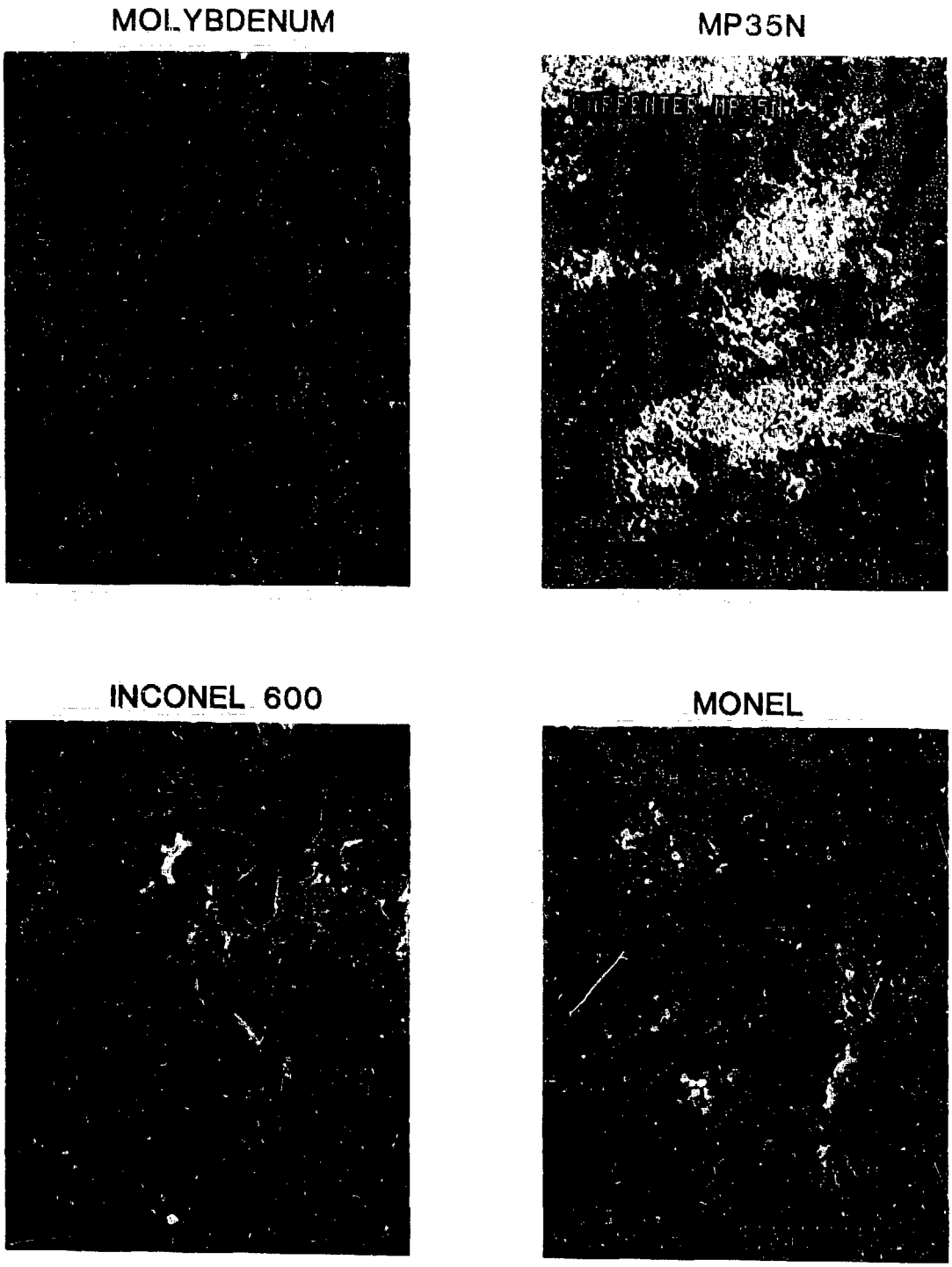

Fig. 4. SEM views of the surfaces of four test coupons.

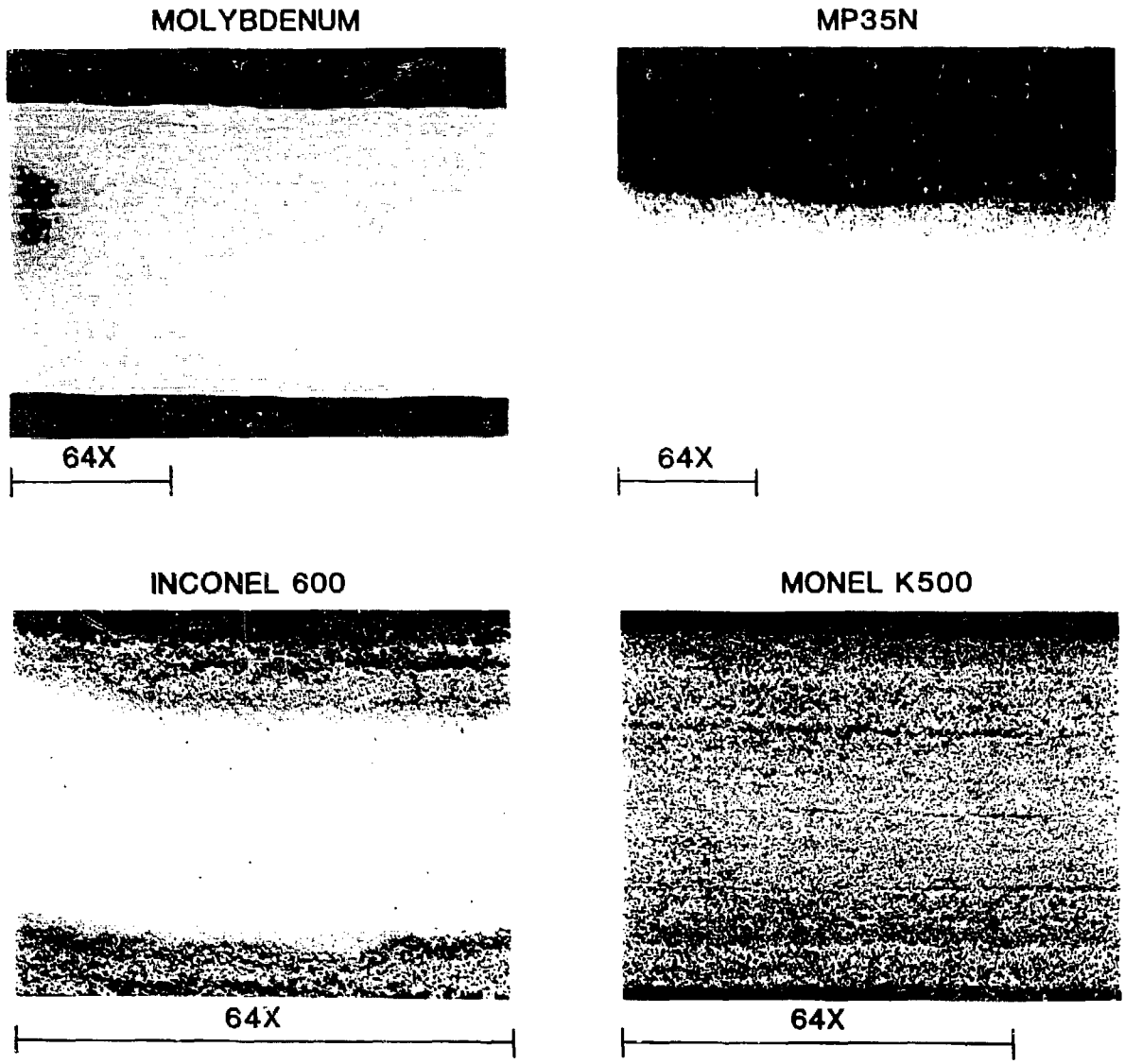

Fig. 5. As-polished cross sections of test coupons show degree of attack. Penetration of attack on molybdenum is zero. Penetration of attack on Monel K500 is 100%.

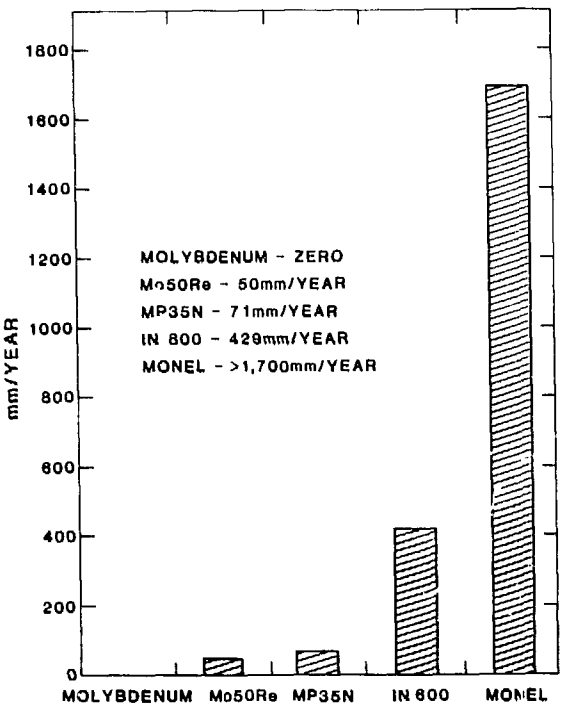

Fig. 6. Rate of attack, as based upon depth-of-penetration data, shown for several samples.

we can reduce their high breakage rates by using different ceramic engineering approaches.

ACKNOWLEDGMENTS

Without the dedicated efforts of many individuals, this project would have suffered greatly. We greatly appreciate the assistance of J. J. Lovato in the laboratory, along with D. W. Anderson and M. J. Chavez, who were invaluable in the early stages of this program. We would like to thank everyone in the Materials Technology Group (MST-6) for their tireless efforts and technical support. Also, the dedication of many individuals in the Analytical Chemistry Group (CHM-1) made possible the volume of analytical data, much of which appears throughout this report.

REFERENCES

1. D. C. Christensen and L. J. Mullins, "Present Status of the Plutonium Metal Production at Los Alamos - 1982," Los Alamos National Laboratory report LA-9674-MS (June 1983).

2. L. J. Mullins, D. C. Christensen, and B. R. Babcock, "Fused Salt Processing of Impure Plutonium Dioxide to High-Purity Plutonium Metal," Los Alamos National Laboratory report LA-9154-MS (January 1982).

3. L. J. Mullins and C. L. Foxx, "Direct Reduction of $^{238}PuO_2$ and $^{239}PuO_2$ to Metal," Los Alamos National Laboratory report LA-9073-MS (February 1982).

4. K. W. Fife, D. F. Bowersox, and E. D. McCormick, "Comparison of Phosgene, Chlorine, and Hydrogen Chloride as Reagents for Converting Molten $CaO \cdot CaCl_2$," Los Alamos National Laboratory report LA-10523-MS (September 1985).

TABLE V

OBSERVATIONS OF COATINGS TESTED
IN THE REGENERATION ENVIRONMENT

Coating	Substrate	Observations
Erbia[a]	Allcorr	Coating completely gone
	ASTM 317L	Coating completely gone
	Hastelloy C276	Coating essentially gone
	Inconel 600	Coating essentially gone
	Inconel 601	Coating completely gone
	Molybdenum	Coating completely gone
Gold[b]	Allcorr	Coating essentially gone
	ASTM 317L	Coating essentially gone
	Hastelloy C276	Coating 95% gone
	Inconel 600	Coating 90% gone
	Inconel 601	Coating completely gone
	Molybdenum	Coating 50% gone
Yttria[c]	Allcorr	Coating 70% gone
	ASTM 317L	Coating 85% gone
	Hastelloy C276	Coating 50% gone
	Inconel 600	Coating 40% gone
	Inconel 601	Coating 40% gone
	Molybdenum	Coating 30% gone
	Ta-10W	Coating 30% gone
	TZM	Coating 60% gone

[a]Data from samples hung 6 in. above the molten salt bath for 1 h.
[b]Data from samples hung 2 in. above the molten salt bath for 1 h.
[c]Data from samples submerged in the molten salt bath for 1 h.

APPENDIX A

ANALYTICAL[a] AND WEIGHT LOSS DATA FOR METALS AND ALLOYS TESTED IN THE REGENERATION ENVIRONMENT.[b]

NICKEL BASE

Allcorr: [Ni + 31 Cr, 10 Mo, 2 W]

Run	Ni	Cr	Mo	W	Weight Loss (g/cm^2)	Cumulative Weight Loss (g/cm^2)
1A	<4	3700	4	<400	0.0182	0.0182
1B	—	—	—	—	0.0199	0.0381
1C	1000	2500	4	<100	0.0336	0.0717
1D	—	—	—	—	0.0384	0.1100
1E	350	6000	<4	<200	0.0429	0.153
1F	—	—	—	—	0.0184	0.171
1G	1500	500	50	<100	0.0182	0.190

Cabot 214: [Ni + 16 Cr, 4.5 Al, 2.5 Fe, Y]

Run	Ni	Cr	Al	Fe	Y	Weight Loss (g/cm^2)	Cumulative Weight Loss (g/cm^2)
1E	60	2000	85	4	<4	0.0105	0.0105
1F	350	7500	60	250	4	0.0109	0.0214
1G	1000	1000	70	150	<4	0.0545	0.0759

Hastelloy B2: [Ni + 28 Mo, 1.6 Fe, 1.0 Cr, 1.0 Co 1 Mn]

Run	Ni	Mo	Fe	Cr	Co	Mn	Weight Loss (g/cm^2)	Cumulative Weight Loss (g/cm^2)
1A	1500	4	120	70	<4	12	0.0296	0.0296
1B	2500	25	350	100	12	20	0.0449	0.0744
1C	—	—	—	—	—	—	0.0422	0.117
1D	2500	250	200	120	4	12	0.0607	0.177
1E	—	—	—	—	—	—	0.0617	0.239
1F	3000	40	100	10	4	6	0.0282	0.267
1G	1000	120	100	12	<4	6	0.0223	0.289

[a] Analytical data are given in parts per million.
[b] Analytical data are from the salt samples taken after each run.

Hastelloy C276: [Ni + 16 Cr, 15 Mo, 5 Fe, 3.7 W, 1.4 Co, 1.0 Mn]

Run	Ni	Cr	Mo	Fe	W	Co	Weight Loss (g/cm^2)	Cumulative Weight Loss (g/cm^2)
1A	1500	600	4	180	<400	<4	0.0164	0.0164
1B	—	—	—	—	—	—	0.0486	0.0650
1C	1500	1000	30	350	<400	150	0.0274	0.0925
1D	—	—	—	—	—	—	0.0576	0.150
1E	—	—	—	—	—	—	0.0767	0.227
1F	1000	400	50	300	<100	50	0.0214	0.248
1G	1000	300	60	900	<100	<4	0.0119	0.260

Hastelloy G3: [Ni + 22 Cr, 19.5 Fe, 7 Mo, 5 Co, 1.5 W, Nb]

Run	Ni	Cr	Fe	Mo	Co	W	Nb	Weight Loss (g/cm^2)	Cumulative Weight Loss (g/cm^2)
1A	—	—	—	—	—	—	—	0.0267	0.0267
1B	25	6100	1200	<4	<4	<100	<40	0.0319	0.0586
1C	—	—	—	—	—	—	—	0.0307	0.0893
1D	600	6000	600	200	50	<100	<40	0.0414	0.131
1E	—	—	—	—	—	—	—	0.0458	0.177
1F	300	200	1200	20	70	<100	<40	0.0062	0.181
1G	600	1000	900	200	<4	<100	<40	0.00342	0.185

Hastelloy S: [Ni + 16 Cr, 15 Mo, 3 Fe, 2 Co, 1 W]

Run	Ni	Cr	Mo	Fe	Co	W	Weight Loss (g/cm^2)	Cumulative Weight Loss (g/cm^2)
1A	2500	2000	<4	120	5	<100	0.0414	0.0414
1B	2500	2000	4	120	10	<100	0.0499	0.0913
1C	2000	3000	85	75	4	<100	0.0106	0.102
1D	250	250	250	30	4	<100	0.0619	0.164
1E	800	2400	<4	30	8	<100	0.117	0.281
1F	400	600	60	40	4	<100	0.0243	0.305
1G	600	1200	20	50	5	<100	0.0579	0.363

Hastelloy X: [Ni + 22 Cr, 18.5 Fe, 9 Mo, 1.5 Co]

Run	Ni	Cr	Fe	Mo	Co	Weight Loss (g/cm^2)	Cumulative Weight Loss (g/cm^2)
1A	40	4900	1200	<4	<4	0.0303	0.0303
1B	—	—	—	—	—	0.0531	0.0834
1C	1000	1200	1500	50	150	0.0396	0.123
1D	—	—	—	—	—	0.0545	0.178
1E	300	5000	1000	30	35	0.0501	0.228
1F	—	—	—	—	—	0.0275	0.25
1G	250	85	60	60	30	0.0181	0.273

Inconel 600: [Ni + 15 Cr, 6 Fe, 1 Mn]

Run	Ni	Cr	Fe	Mn	Weight Loss (g/cm^2)	Cumulative Weight Loss (g/cm^2)
2A	30	50	250	25	0.00031	0.00031
2B	20	600	100	12	0.0081	0.0084
2C	200	2000	500	20	0.0408	0.0492
2D	120	1000	400	15	0.0105	0.0596
2E	120	1200	600	15	0.0269	0.0866
2F	250	1800	350	25	0.0307	0.1170
2G	300	2500	600	25	0.0323	0.150
2H	180	2500	850	25	0.0324	0.182

Inconel 601: [Ni + 23 Cr, 14 Fe, 1.5 Al, Mn]

Run	Ni	Cr	Fe	Al	Mn	Weight Loss (g/cm^2)	Cumulative Weight Loss (g/cm^2)
2A	6	1200	85	85	25	0.000385	0.00385
2B	—	—	—	—	—	0.0181	0.0185
2C	10	3000	60	15	25	0.0339	0.0524
2D	60	3000	600	6	40	0.0312	0.0836
2E	50	3000	600	120	25	0.0208	0.104
2F	85	3000	500	85	25	0.0160	0.120
2G	250	1800	600	30	18	0.0258	0.146

Inconel 617: [Ni + 22 Cr, 12.5 Co, 9 Mo, 1.5 Fe,1 Al]

Run	Ni	Cr	Co	Mo	Fe	Al	Weight Loss (g/cm^2)	Cumulative Weight Loss (g/cm^2)
1A	230	600	180	<10	50	25	0.0182	0.0182
1B	720	—	300	<10	100	12	0.0214	0.0397
1C	430	850	250	<10	65	40	0.0149	0.0546
1D	760	850	250	<10	65	18	0.0152	0.0698
1E	840	1200	300	<10	80	25	0.00185	0.0716
1F	450	1200	300	12	250	25	0.0155	0.0871

Inconel 625: [Ni + 20 Cr, 9 Mo, 5 Fe, 4 (Nb + Ta)]

Run	Ni	Cr	Mo	Fe	Ta	Nb	Weight Loss (g/cm^2)	Cumulative Weight Loss (g/cm^2)
1A	—	—	—	—	—	—	0.00399	0.00399
1B	600	3500	25	1000	<100	<40	0.0335	0.0375
1C	—	—	—	—	—	—	0.0568	0.0944
1D	1200	1200	10	250	<100	<40	0.0398	0.134
1E	—	—	—	—	—	—	0.0476	0.182
1F	1000	6000	35	250	<100	35	0.0175	0.199
1G	750	1500	30	350	<100	<40	0.0426	0.242

Inconel 690: [Ni + 30 Cr, 9 Fe]

Run	Ni	Cr	Fe	Weight Loss (g/cm^2)	Cumulative Weight Loss (g/cm^2)
1A	17	2250	8	0.0139	0.0139
1B	13	2250	7	0.0100	0.0239
1C	10	1800	25	0.00971	0.0337
1D	260	>1000	550	0.0623	0.0960
1E	—	—	—	0.00158	0.0975
1F	—	—	—	0.0353	0.133

Inconel 750: [Ni + 14 Cr, 5 Fe, 2.5 Ti, Nb]

Run	Ni	Cr	Fe	Ti	Nb	Weight Loss (g/cm^2)	Cumulative Weight Loss (g/cm^2)
1A	350	1200	370	10	<40	0.0186	0.0186
1B	330	500	200	4	<40	0.00741	0.0260
1C	200	7	110	25	<40	0.00002	0.0260
1D	1200	1000	500	6	<40	0.0496	0.0757
1E	1000	1000	340	6	<40	0.00424	0.0799
1F	400	60	100	20	<40	0.0238	0.1037

Inconel 751: [Ni + 14 Cr, 5 Fe, 2 Ti, 1 Al, Nb]

Run	Ni	Cr	Fe	Ti	Al	Nb	Weight Loss (g/cm^2)	Cumulative Weight Loss (g/cm^2)
1A	300	1000	250	4	25	<10	0.0336	0.0336
1B	80	850	110	18	25	<10	0.0254	0.0589
1C	220	1000	260	18	25	<10	0.0564	0.115
1D	470	300-3000	390	10	40	<10	0.0559	0.171
1E	420	300-3000	390	12	40	<10	0.0634	0.235
1F	800	1200	370	12	60	<10	0.0397	0.274

Monel K500: [Ni + 30 Cu, 3 Al, 1 Fe]

Run	Ni	Cu	Al	Fe	Weight Loss (g/cm^2)	Cumulative Weight Loss (g/cm^2)
1A	180	1200	10	40	0.0248	0.0248
1B	30	4000	100	25	0.0300	0.0548
1C	25	4000	100	25	0.0179	0.0727
1D	20	2500	300	25	0.0104	0.0831
1E	40	4000	60	25	0.0178	0.101
1F	180	5000	100	60	0.0212	0.122

IRON BASE

ASTM 317L: [Fe + 18.4 Cr, 15.8 Ni, 4.2 Mo, 1.6 Mn, 0.4 Cu]

Run	Fe	Cr	Ni	Mo	Mn	Weight Loss (g/cm^2)	Cumulative Weight Loss (g/cm^2)
1A	1800	4300	<4	<4	150	0.0378	0.0378
1B	—	—	—	—	—	0.0257	0.0636
1C	4900	2500	25	<4	120	0.0288	0.0924
1D	—	—	—	—	—	0.0303	0.123
1E	2500	2500	600	250	85	0.0247	0.147
1F	—	—	—	—	—	0.0194	0.167
1G	2000	600	50	30	100	0.0186	0.185

ASTM A446: [Fe + 25 Cr, 0.6 Mn, 0.4 Ni, Si]

Run	Fe	Cr	Mn	Ni	Si	Weight Loss (g/cm^2)	Cumulative Weight Loss (g/cm^2)
1A	600	2500	25	25	180	0.0282	0.0282
1B	3700	3700	40	25	—	0.0423	0.0705
1C	—	—	—	—	—	0.0496	0.120
1D	2000	2000	50	30	100	0.0553	0.175
1E	2000	2500	35	<4	350	0.0857	0.261
1F	—	—	—	—	—	0.0286	0.290
1G	1000	1500	30	4	300	0.0271	0.317

COBALT BASE

Carpenter L605: [Co + 20 Cr, 15 W, 10 Ni]

Run	Co	Cr	W	Ni	Weight Loss (g/cm^2)	Cumulative Weight Loss (g/cm^2)
1A	100	250	<400	55	0.00664	0.00664
1B	600	—	<400	55	0.0225	0.0292
1C	1200	1200	<400	100	0.0281	0.0573
1D	1200	1000	<400	150	0.0261	0.0834
1E	1200	1000	<400	180	0.0273	0.111
1F	1200	1000	<400	140	0.0306	0.141

MP35N: [Co + 35 Ni, 20 Cr, 10 Mo]

Run	Co	Ni	Cr	Mo	Weight Loss (g/cm^2)	Cumulative Weight Loss (g/cm^2)
1A	1000	250	1200	12	0.0287	0.0287
1B	—	—	—	—	0.0265	0.0551
1C	—	—	—	—	0.00297	0.0581
1D	—	—	—	—	0.0159	0.0740
1E	200	100	60	400	0.00576	0.0797
1F	100	200	50	100	0.0442	0.1239

REFRACTORY BASE

ASTM B708: [Ta + 2.5 W, 0.15 Nb]

Run	Ta	W	Nb	Weight Loss (g/cm^2)	Cumulative Weight Loss (g/cm^2)
1A	<120	350	<35	0.00365	0.00365
1B	15000	100	<40	0.126	0.129
1C	12000	100	<40	0.250	0.379

KBI 40: [Ta + 40 Nb]

Run	Ta	Nb	Weight Loss (g/cm^2)	Cumulative Weight Loss (g/cm^2)
1A	<120	<35	0.0175	0.0175
1B	25000	25000	0.209	0.227

Moly-10Re [Mo + 10 Re]

Run	Mo	Re	Weight Loss (g/cm^2)	Cumulative Weight Loss (g/cm^2)
1A	<4	<40	0.00449	0.00449
1B	<4	<40	0.00385	0.00834
1C	<4	<40	0.00353	0.0119
1D	<4	<40	0.00448	0.0167
1E	<4	<40	0.00437	0.0211
1F	<4	<40	0.00767	0.0287
1G	6	<40	0.00438	0.0331

Moly-50Re [Mo + 50 Re]

Run	Mo	Re	Weight Loss (g/cm^2)	Cumulative Weight Loss (g/cm^2)
1A	—	—	0.00489	0.00489
1B	<4	<40	0.00682	0.0117
1C	<4	<40	0.00664	0.0184
1D	<4	<40	0.00930	0.0277
1E	<4	<40	0.00963	0.0373
1F	<4	<40	0.0117	0.0490

Ta-10W. [Ta + 10 W]

Run	Ta	W	Weight Loss (g/cm^2)	Cumulative Weight Loss (g/cm^2)
1A	<120	<350	0.0063	0.0063
1B	2500	<400	0.0778	0.0845
1C	2500	250	0.0953	0.1798
1D	400	<400	0.1067	0.2865

TZM: [Mo + 0.5 Ti, 0.1 Zr]

Run	Mo	Ti	Zr	Weight Loss (g/cm^2)	Cumulative Weight Loss (g/cm^2)
1A	500	<4	<10	0.0261	0.0261
2B	—	—	—	0.0113	0.0374
1C	600	6	<12	0.00949	0.0469
1D	—	—	—	0.0701	0.117
1E	—	—	—	0.0132	0.130
1F	50	—	—	0.0167	0.147
1G	20	—	—	0.0140	0.161

ZIRCONIUM BASE

Zirconium 705: [Zr + 4.0 Hf, 2.5 Nb, Oxygen]

Run	Zr	Hf	Nb	Weight Loss (g/cm^2)	Cumulative Weight Loss (g/cm^2)
1A	120	<100	<40	0.00438	0.00438
1B	250	<100	<40	0.0117	0.0161
1C	300	<100	<40	0.0112	0.0272
1D	<10	<100	<40	0.0267	0.0540
1E	250	<100	<40	0.0560	0.1100
1F	200	<100	<40	0.00779	0.1178

Zircaloy 4: [Zr + 4.0 Hf, 1.5 Sb, 0.2 Fe, 0.1 Cr, Oxygen]

Run	Zr	Hf	Fe	Cr	Weight Loss (g/cm^2)	Cumulative Weight Loss (g/cm^2)
1A	18	<100	10	4	0.00216	0.00216
1B	180	<100	85	6	0.00231	0.00447
1C	120	<100	10	<4	0.0104	0.0148
1D	250	<100	<4	<4	0.00227	0.0171
1E	850	<100	25	<4	0.0159	0.0330
1F	1000	<100	<4	<4	0.0101	0.0431

PURE METALS

Cobalt: [Co]

Run	Co	Weight Loss (g/cm^2)	Cumulative Weight Loss (g/cm^2)
1A	—	0.242	0.242
1B	<4	0.0590	0.302
1C	<4	0.0656	0.367
1D	<4	0.0760	0.443
1E	<4	0.0786	0.522
1F	100	0.0303	0.552

Hafnium: [Hf + 4 Zr] (After this run, 50% of the sample was lost.)

Run	Hf	Zr	Weight Loss (g/cm^2)	Cumulative Weight Loss (g/cm^2)
1A	<450	<10	0.0198	0.0198

Molybdenum: [Mo]

Run	Co	Weight Loss (g/cm^2)	Cumulative Weight Loss (g/cm^2)
1A	400	0.0143	0.0143
1B	<4	0.0117	0.0261
1C	25	0.00926	0.0353
1D	2000	0.0155	0.0508
1E	30	0.00958	0.0604
1F	250	0.00937	0.0697
1G	25	0.0112	0.0809
1H	40	0.0132	0.0942
1I	<4	0.00745	0.102

Nickel: [Ni]

Run	Ni	Weight Loss (g/cm^2)	Cumulative Weight Loss (g/cm^2)
1A	20100	0.0283	0.0283
1B	4100	0.100	0.128
1C	2900	0.0678	0.196
1D	2500	0.0942	0.290
1E	3600	0.0663	0.357

Rhenium: [Re]

Run	Re	Weight Loss (g/cm^2)	Cumulative Weight Loss (g/cm^2)
1A	<40	0.000226	0.000226
1B	<40	0.00672	0.00694
1C	<40	0.0119	0.0188
1D	—	0.000366	0.0192
1E	<40	0.00157	0.0207
1F	<40	0.00181	0.0225
1G	<40	0.00129	0.0238

Tantalum: [Ta]

Run	Ta	Weight Loss (g/cm^2)	Cumulative Weight Loss (g/cm^2)
1A	<120	0.00271	0.00271
1B	500	0.0896	0.0923
1C	500	0.110	0.203
1D	500	0.148	0.351
1E	25000	0.158	0.509
1F	12000	0.132	0.640

Titanium: [Ti] (After this run, 80% of the sample was lost.)

Run	Ti	Weight Loss (g/cm^2)	Cumulative Weight Loss (g/cm^2)
1A	380	0.0916	0.0916

Tungsten: [W]

Run	W	Weight Loss (g/cm^2)	Cumulative Weight Loss (g/cm^2)
1A	<350	0.00684	0.00684
1B	<400	0.167	0.174
1C	—	0.168	0.342
1D	370	0.171	0.512
1E	250	0.110	0.622
1F	<400	0.122	0.744
1G	<400	0.056	0.800
1H	<400	0.066	0.867
1I	100	0.105	0.972

Zirconium: [Zr]

Run	Zr	Weight Loss (g/cm^2)	Cumulative Weight Loss (g/cm^2)
1A	370	0.0179	0.0179
1B	120	0.0238	0.0417
1C	300	0.0447	0.0864
1D	200	0.00551	0.0919

APPENDIX B

ANALYTICAL[a] AND WEIGHT LOSS DATA FOR METALS AND ALLOYS TESTED IN THE REGENERATION ENVIRONMENT.[b]

$Al_2O_3 + 2\% Y_2O_3$

Run	Al	Y	Mg	Li	Weight Loss (g/cm^2)	Cumulative Weight Loss (g/cm^2)
1A	1000-2000	40	260		0.193	0.193
1B	—	—	—	—	0.00985	0.203
1C	1200	40	350	260	0.288	0.491
1D	400-4000	60	370	260	0.0233	0.514
1E	400-4000	60	340	260	0.0396	0.554
1F	600	40	400	180	0.0312	0.585

BeO

Run	Be	Weight Loss (g/cm^2)	Cumulative Weight Loss (g/cm^2)
1A	—	0.000897	0.000897
1B	25	0.000812	0.00171
1C	50	0.000952	0.00266
1D	—	0.000360	0.00302

Ce_2S (Sample was completely consumed.)

Run	Weight Loss (g/cm^2)	Cumulative Weight Loss (g/cm^2)
1A	All	All

[a]Analytical data are given in parts per million.
[b]Analytical data are from salt samples taken after each run.

$MgO + Al_2O_3$

Run	Mg	Al	Li	Si	Weight Loss (g/cm^2)	Cumulative Weight Loss (g/cm^2)
1A	600	1200	180	700	0.0568	0.0568
1B	—	—	—	—	0.0697	0.126
1C	—	—	—	—	0.0701	0.197
1D	270	100	230	600	—	—
1E	—	—	—	—	0.0928	0.289
1F	630	1000	270	370	0.108	0.397

$MgO + 1\% Y_2O_3$

Run	Mg	Y	Li	Weight Loss (g/cm^2)	Cumulative Weight Loss (g/cm^2)
1A	—	—	—	0.284	0.284
1B	3200	100	170	0.234	0.518
1C	1400	60	160	0.0915	0.610
1D	1100	40	170	0.0672	0.677
1E	1300	10	200	0.0887	0.766
1F	1450	60	260	0.0793	0.845

$MgO + 3\% Y_2O_3$

Run	Mg	Y	Al	Weight Loss (g/cm^2)	Cumulative Weight Loss (g/cm^2)
1A	510	<4	25	0.265	0.265
1B	1900	<25	30	0.706	0.971
1C	850	<10	30	0.0308	1.002
1D	900	<10	25	0.0369	1.039
1E	1700	6	25	0.0823	1.121
1F	1900	50	60	0.0885	1.210

SiC

Run	Si	Li	Mg	Weight Loss (g/cm^2)	Cumulative Weight Loss (g/cm^2)
1A	200	160	400	0.00462	0.00462
1B	100	170	250	0.125	0.129
1C	300	160	280	0.0835	0.213
1D	100	160	250	0.0478	0.261
1E	800	200	200	0.0420	0.303
1F	3000	200	80	0.0427	0.345

ThO_2

Run	Al	Si	Weight Loss (g/cm^2)	Cumulative Weight Loss (g/cm^2)
1A	25	350	—	—
1B	60	600	0.421	0.421
1C	25	600	0.346	0.767

$ZrO_2 + 15\%\ Y_2O_3$: (Two samples run; both broke after one run.)

Run	Zr	Y	Si	Weight Loss (g/cm^2)	Cumulative Weight Loss (g/cm^2)
1A	<10	100	400	0.00557	0.00557
1B	—	—	—	0.0159	0.0159